Focusing through dynamic scattering media

C. Stockbridge,[1] Y. Lu,[1] J. Moore,[2] S. Hoffman,[1] R. Paxman,[3] K. Toussaint,[1] and T. Bifano[1,*]

[1]*Department of Mechanical Engineering, Boston University, 110 Cummington St. Boston, Massachusetts 02215, USA*
[2]*Department of Electrical Engineering, Boston University, 8 Saint Mary's St. Boston, Massachusetts 02215, USA*
[3]*Paxman Consulting, 9228 Sunset Lake Dr., Saline, Michigan 48176, USA*
[4]*University of Illinois at Urbana-Champaign, 1206 W. Green St., Urbana, Illinois 61801, USA*
[*] *tgb@bu.edu*

Abstract: We demonstrate steady-state focusing of coherent light through dynamic scattering media. The phase of an incident beam is controlled both spatially and temporally using a reflective, 1020-segment MEMS spatial light modulator, using a coordinate descent optimization technique. We achieve focal intensity enhancement of between 5 and 400 for dynamic media with speckle decorrelation time constants ranging from 0.4 seconds to 20 seconds. We show that this optimization approach combined with a fast spatial light modulator enables focusing through dynamic media. The capacity to enhance focal intensity despite transmission through dynamic scattering media could enable advancement in biological microscopy and imaging through turbid environments.

OCIS codes: (290.4210) Multiple scattering; (010.1080) Active or adaptive optics; (110.0113) Imaging through turbid media; (230.6120) Spatial light modulators; (230.3990) Micro-optical devices.

References and links

1. I. M. Vellekoop and C. M. Aegerter, "Scattered light fluorescence microscopy: imaging through turbid layers," Opt. Lett. **35**(8), 1245–1247 (2010).
2. I. M. Vellekoop and A. P. Mosk, "Focusing coherent light through opaque strongly scattering media," Opt. Lett. **32**(16), 2309–2311 (2007).
3. I. Vellekoop, A. Lagendijk, and A. Mosk, "Exploiting disorder for perfect focusing," Nat. Photonics **4**(5), 320–322 (2010).
4. G. Montaldo, M. Tanter, and M. Fink, "Time reversal of speckle noise," Phys. Rev. Lett. **106**(5), 054301 (2011).
5. S. M. Popoff, G. Lerosey, R. Carminati, M. Fink, A. C. Boccara, and S. Gigan, "Measuring the Transmission Matrix in Optics: An Approach to the Study and Control of Light Propagation in Disordered Media," Phys. Rev. Lett. **104**(10), 100601 (2010).
6. S. Popoff, G. Lerosey, M. Fink, A. C. Boccara, and S. Gigan, "Image transmission through an opaque material," Nat Commun **1**(6), 81 (2010).
7. G. Lerosey, J. de Rosny, A. Tourin, and M. Fink, "Focusing beyond the diffraction limit with far-field time reversal," Science **315**(5815), 1120–1122 (2007).
8. I. Vellekoop and C. Aegerter, "Focusing light through living tissue," San Francisco, California, USA, SPIE **7554**, 755430 (2010).
9. D. B. Conkey, A. M. Caravaca-Aguirre, and R. Piestun, "High-speed scattering medium characterization with application to focusing light through turbid media," Opt. Express **20**(2), 1733–1740 (2012).
10. T. Bifano, "Adaptive imaging: MEMS deformable mirrors," Nat. Photonics **5**(1), 21–23 (2011).
11. K. Baker, E. Stappaerts, D. Homoelle, M. Henesian, E. Bliss, C. Siders, and C. Barty, "Interferometric adaptive optics for high-power laser pointing and wavefront control and phasing," J. Micro/Nano, MEMS and MOEMS **8**(3), 033040 (2009).
12. K. Baker, E. Stappaerts, D. Gavel, S. Wilks, J. Tucker, D. Silva, J. Olsen, S. Olivier, P. Young, M. Kartz, L. Flath, P. Kruelivitch, J. Crawford, and O. Azucena, "High-speed horizontal-path atmospheric turbulence correction using a large actuator-number MEMS spatial light modulator in an interferometric phase conjugation engine," Opt. Lett. **29**, 1781–1783 (2004).
13. N. Kasdin, R. Vanderbei, and R. Belikov, "Shaped pupil coronagraphy," C. R. Phys. **8**(3-4), 312–322 (2007).
14. R. Belikov, E. Pluzhnik, M. Connelley, F. Witteborn, D. Lynch, K. Cahoy, O. Guyon, T. Greene, and M. McKelvey, "First results on a new PIAA coronagraph testbed at NASA Ames," *Techniques and Instrumentation for Detection of Exoplanets IV* (San Diego, Calif., 2009) Proc. SPIE **7440**, 74400J (2009).
15. R. Belikov, E. Pluzhnik, M. Connelley, F. Witteborn, T. Greene, D. Lynch, P. Zell, and O. Guyon, "Laboratory demonstration of high-contrast imaging at 2 lambda/D on a temperature-stabilized testbed in air," *Space*

#168050 - $15.00 USD Received 9 May 2012; revised 7 Jun 2012; accepted 7 Jun 2012; published 20 Jun 2012

Telescopes and Instrumentation 2010: Optical, Infrared, and Millimeter Wave (San Diego, Calif., 2011) Proc. SPIE **7731**, D1–D11 (2011).
16. S. Thomas, R. Soummer, D. Dillon, B. Macintosh, D. Gavel, and A. Sivaramakrishnan, "Testing the apodized pupil Lyot coronagraph on the laboratory for adaptive optics extreme adaptive optics testbed," Astron. J. **142**(4), 119 (2011).
17. S. Thomas, R. Soummer, D. Dillon, B. Macintosh, J. Evans, D. Gavel, A. Sivaramakrishnan, C. Marois, and B. Oppenheimer, "Testing the APLC on the LAO ExAO testbed," *Adaptive Optics Systems* (Marseille, France 2008) SPIE **7015**, 70156I (2008).
18. B. Macintosh, J. Graham, D. Palmer, R. Doyon, D. Gavel, J. Larkin, B. Oppenheimer, L. Saddlemyer, J. Wallace, B. Bauman, D. Erikson, L. Poyneer, A. Sivaramakrishnan, R. Soummer, and J. Veran, "Adaptive optics for direct detection of extrasolar planets: the Gemini Planet Imager," C. R. Phys. **8**(3-4), 365–373 (2007).
19. D. Gavel, S. Severson, B. Bauman, D. Dillon, M. Reinig, C. Lockwood, D. Palmer, K. Morzinski, M. Ammons, E. Gates, and G. Grigsby, "Villages: an on-sky visible wavelength astronomy AO experiment using a MEMS deformable mirror," Proc. SPIE MEMS Adaptive Optics II **6888**, 688804–688807 (2008).
20. F. Wang, "Control of deformable mirror with light-intensity measurements through single-mode fiber," Appl. Opt. **49**(31), G60–G66 (2010).
21. F. Wang, "Wavefront sensing through measurements of binary aberration modes," Appl. Opt. **48**(15), 2865–2870 (2009).
22. F. Wang, "Utility transforms of optical fields employing deformable mirror," Opt. Lett. **36**(22), 4383–4385 (2011).
23. F. Wang, "High-contrast imaging via modal convergence of deformable mirror," Astrophys. J. **751**(2), 83 (2012).
24. J. Walsh, "A closed set of normal orthogonal functions," Am. J. Math. **45**(1), 5–24 (1923).
25. H. Schreiber and J. Bruning, *Optical Shop Testing* (John Wiley & Sons, Inc., 2006), Chap. 15.
26. I. Vellekoop and A. Mosk, "Phase control algorithms for focusing light through turbid media," Opt. Commun. **281**(11), 3071–3080 (2008).
27. F. Helmchen and W. Denk, "Deep tissue two-photon microscopy," Nat. Methods **2**(12), 932–940 (2005).

1. Introduction

A number of research groups have demonstrated optical focusing through stationary scattering media [1–7] using either coordinate descent optimization or measurement of the system's effective transmission matrix. Either approach controls phase of a beam incident on a scattering medium using a liquid crystal spatial light modulator (SLM), with a goal of optimizing intensity at a point on the opposite side of the medium. An optical intensity sensor provides control feedback. In coordinate descent optimization focus intensity is optimized iteratively for each of N input modes where N corresponds to the number of spatial degrees of freedom in the SLM. In transmission matrix optimization the relationship between optical input and output modes of the system is estimated from an ensemble of N SLM input states and N corresponding output states. Using that relationship one can optimize focus at any point in the measured field. Moreover, one can use the estimated transmission matrix to predict the SLM input state that will optimize an arbitrary output state. We believe that coordinate descent optimization should be advantageous for focusing through a *dynamic* medium since that approach continuously adapts to the changing medium state with each new measurement, whereas the transmission matrix optimization can only adapt after an ensemble of measurements. The ability to focus light through highly scattering media could enable improvements in biological microscopy in biological tissue. A nontrivial challenge associated with this in most applications, however, is the dynamic nature of scattering in such tissue, or conversely, the strong sensitivity of the transmission matrix on the precise geometry of the system. Micrometer-scale translations of the medium or the beam almost completely eliminate focal intensity enhancements that required hundreds or thousands of control iterations to establish.

More recently this technique has been extended to steady focusing light through a slowly evolving dynamic biological medium with decorrelation time constants of twenty-five seconds [8], and intermittent focusing through a more highly scattering media with decorrelation time constants less than one second [9]. Because the latter work involved calculating a transmission matrix and then freezing the SLM state to provide focus, the enhancement deteriorated within a period comparable to the speckle decorrelation time.

In this paper we report on steady focusing enhancement over a wide range of decorrelation time constants, including sub-second time constants. We also quantify focusing enhancement as a function of number of degrees of freedom in the SLM. We have taken an additional step

#168050 - $15.00 USD Received 9 May 2012; revised 7 Jun 2012; accepted 7 Jun 2012; published 20 Jun 2012

in dynamic optimization by using a high-speed segmented MEMS deformable mirror [Boston Micromachines Corporation, Kilo-SLM] [10] spatial light modulator (SLM) to maintain highly enhanced focus through media having speckle decorrelation time constants consistent with those of typical biological tissue.

2. Experimental apparatus

The Kilo-SLM has been used previously in a variety of applications requiring control of dynamic aberrations containing high spatial and/or temporal frequencies [11–19]. It is comprised of 1020 mirror segments in a 32 × 32 array where the 4 corner segments are fixed. Each segment measures 300μm square and 3μm thick and can be translated in a surface-normal direction using voltage control to an underlying electrostatic actuator. Each segment's surface-normal translation is controllable over a range of ~1.5μm, except for the four immovable corner segments. The SLM was pre-calibrated using a surface mapping interferometer [Zygo NewView 6300], to allow subsequent direct phase control with ~0.01 wave accuracy at the laser wavelength of 532nm. The SLM can be updated at a frame rate of >10kHz. In the experiments reported here, the 32 × 32 pixel CMOS sensor [USB 2 uEye LE] used for optimization feedback limited the overall system control frequency to ~330Hz. Control frequency is defined as the frequency at which the SLM can be updated and the sensor read.

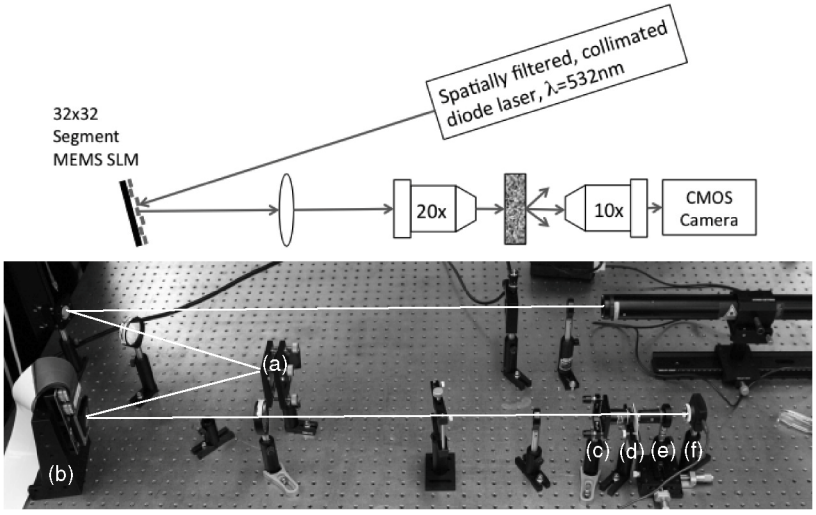

Fig. 1. Schematic of the experimental apparatus. A collimated, spatially filtered laser beam, (a), reflects from the SLM surface, (b), acquiring a spatially distributed phase shift. The wavefront at the SLM is reimaged by a 45 × telescope comprised of a 400mm focal length lens and a 20 × , 0.4NA microscope objective, (c) onto the near side of the scattering medium, (d). A microscope objective on the far side of the scattering medium, (e), projects a portion of the resulting speckle pattern onto a fixed detector, (f).

A schematic representation and a photograph of the experimental setup are depicted in Fig. 1. The phase of a collimated beam can be controlled over a full wavelength at each of the spatially distributed, independent mirror segments. The SLM optical plane is reimaged onto the front surface of a scattering medium using a lens and a microscope objective, and scattered light exiting the medium is projected by a second microscope objective onto the CMOS camera sensor. The goal of the optimization algorithm is to maximize the intensity of a single speckle grain in the camera sensor plane.

3. Optimization algorithm

The optimization algorithm employed in this work is based on coordinate descent using 1024 orthogonal 2D Walsh functions as a basis set [20–23]. Each 2D Walsh function, W_k, has 32 ×

#168050 - $15.00 USD Received 9 May 2012; revised 7 Jun 2012; accepted 7 Jun 2012; published 20 Jun 2012

32 (1024) terms that are bi-valued (+ 1 or −1). Each term is associated with a corresponding mirror segment in the 32 × 32 SLM [24]. A collection of 1024 Walsh matrices scaled by corresponding coefficients a_k (in units of waves) represents an orthogonal basis set for the 1020 segment SLM. For simplicity, we ignore the fact that the four corner segments of the SLM are not functional. All possible states can be produced using a linear combination of scaled Walsh functions.

To implement Walsh optimization, the modal coefficient a_k of each Walsh function W_k is adjusted sequentially to maximize the scalar optimization metric S, defined in our experiments as the intensity of a selected pixel on the camera (In all of our experiments, pixel coordinate 16,16 near the center of our 32 × 32 camera sensor was selected). For a particular Walsh mode, k, an initial measure is made of the optimization metric, S_{k0}, with a modal coefficient of 0. Next, the modal coefficient of the Walsh function is set to a prescribed value $+\alpha$, (typically, but not necessarily, ¼ of a wave), and a scalar measure (S_{k1}) of the optimization metric is made. Next, the modal coefficient of the Walsh function is set to a prescribed value $-\alpha$ and a third scalar measure (S_{k2}) of the desired optimization metric is made. Finally, the coordinate optimal value for this Walsh function coefficient (in waves) is calculated using a standard technique for three-point phase shifting interferometry [25]:

$$a_k = \tan^{-1}\left[\frac{\left(S_{k2} - S_{k1}\right)\tan\left(\frac{\pi}{\alpha}\right)}{2S_{k0} - S_{k1} - S_{k2}}\right] \tag{1}$$

The process is repeated for all 1024 Walsh coordinate functions. Because each Walsh coordinate optimization requires three perturbations (i.e. three sequences of SLM output followed by camera input), the effective optimization frequency for Walsh coordinate optimization is one third of the base control frequency, or ~110Hz.

4. Experimental results

In a qualitative demonstration of the technique, focus was enhanced through an *ex vivo* 5mm thick section of chicken breast. Before optimization, the decorrelation time constant of the speckle at the camera was measured to be 3.4s, based on an ensemble average autocorrelation for each pixel in the 32x32 pixel camera array decaying to the 3dB point. Figure 2 illustrates the results. Focus enhancement, normalized by the mean camera intensity prior to optimization, reached approximately 160 with a standard deviation of 15, and did not diminish while the optimization controller continued to run for nearly two minutes. After the controller was stopped, with the SLM fixed at its final state, the enhancement dropped to a normalized value of ~1 with an enhancement decay time constant measured to be 3.6s – approximately the same as the sample decorrelation time.

This result suggests, as expected, that the decay time after optimization corresponds to the speckle decorrelation time before optimization. It is expected that the peak enhancement would be smaller for optimization through media characterized by shorter speckle decorrelation times, and *vice versa*, given a fixed controller update rate.

#168050 - $15.00 USD Received 9 May 2012; revised 7 Jun 2012; accepted 7 Jun 2012; published 20 Jun 2012

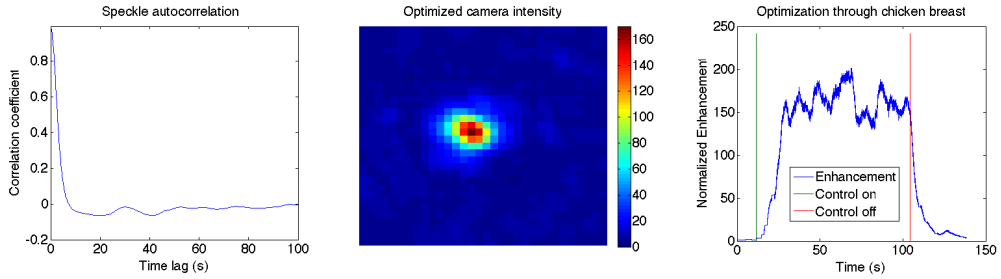

Fig. 2. Experimental results for focus optimization though a 5mm *ex vivo* sample of chicken breast tissue. Before each optimization, the mean intensity on the camera was measured. This value was then used as a normalization constant for subsequent enhancement measurements. Left: Ensemble average autocorrelation for the fully developed speckle pattern on the camera prior to optimization. The decorrelation time constant was estimated to be ~3.4s from this data. Center: Optimized focus spot centered on the pixel at coordinate location (16,16) within the 32-pixel square camera sensor area, with peak intensity ~160 times larger than the initial mean camera intensity measured within this area. Right: Normalized peak intensity on the camera as a function of time before, during, and after optimization. After optimization is stopped, the focus enhancement decays with a first-order time constant of ~3.6s to the background intensity level. A similar plot in Media 1 shows the full progression of the enhancement along with the real time decay using a sample composed of polystyrene spheres translating at 200µm per second.

To quantify system performance as a function of media-dependent speckle decorrelation time, an experiment was conducted in which optimization was performed through a medium comprised of two axially sequential adjacent cuvettes containing identical media. The first cuvette traversed the beam axis at fixed speed while the second cuvette remained stationary. The medium was comprised of 0.75µm diameter polystyrene spheres (Polybead® Microspheres) diluted to a concentration of 0.125% by volume and suspended in agarose gel. At this dilution the medium has a transport mean free path – the distance over which the direction of propagation becomes randomized – of 4mm. The first cuvette was 4mm thick and the second was 1.2mm thick. The speckle pattern produced by a beam passing through these two samples was fully developed, and had a decorrelation time that scaled in proportion to the speed of the translating sample. Sample translation was generated using a piezoelectric actuator, and speed was measured by differentiating the output of a linear variable differential transformer (LVDT) displacement gage. Translation speeds ranging from 75nm/s to 3µm/sec were used in these experiments, yielding measured speckle decorrelation times of 0.35s to 18s. Prior to conducting the dynamic experiments, focus was optimized through the combined media without translation. Peak normalized enhancement after optimization in this stationary case was approximately 380 with a standard deviation of ~20. For all dynamic experiments, optimization duration was 90s. Peak focus enhancement for translating media ranged from a low of 5 at a translation speed of 3µm/s, corresponding to a speckle decorrelation time of 0.4s, to a high of 380 at a translation speed of 75nm/s, corresponding to a speckle decorrelation time of 20s. Figure 3 illustrates the optimization results graphically for a number of dynamic conditions using 1020 independent SLM segments in the optimization.

If we consider the speckle evolution and the optimization to be competing first-order processes characterized by their respective time constants, we can estimate the expected peak enhancement can be made as a function of the number of independent segments in the SLM, N, the time required to update each Walsh term in the optimization process T_i, (0.085s for the present system) and the speckle decorrelation time T_d, and a proportionality constant α. That relationship adapted from [2] is as follows:

$$E = \frac{\alpha N}{\left(1 + \frac{NT_i}{T_d}\right)} \tag{2}$$

#168050 - $15.00 USD Received 9 May 2012; revised 7 Jun 2012; accepted 7 Jun 2012; published 20 Jun 2012

In the case of a static medium, this reduces to $E = \alpha N$. In our static medium experiments we found that α~0.5, a constant of proportionality similar to that achieved experimentally by other researchers using liquid crystal SLMs [2, 8]. The theoretical maximum for α proposed in [2] is $\pi/4$.

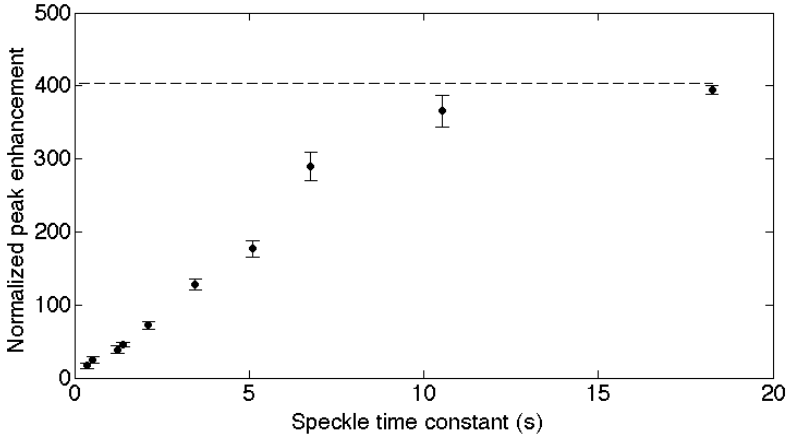

Fig. 3. Peak optimized enhancement measured as a function of initial speckle decorrelation time for a dynamic scattering medium, with Walsh function coordinate optimization update rate of 110Hz and 1020 phase-modulating segments. The dashed line corresponds to the mean peak enhancement level achieved when the medium was stationary. Error bars correspond to one standard deviation of enhancement fluctuation over a 10s period at the end of the optimization trial.

We conducted a series of experiments similar to those shown in Fig. 3, but using fewer independent segments in the SLM and correspondingly fewer Walsh coordinate functions in the optimization algorithm. The optics of the system were not changed: to reduce the number of independent segments, the mirrors segments in the SLM were grouped into dependent clusters of 2x2 4x4 and 8x8 "super-segments" corresponding to effective SLM array sizes of 256, 64, and 16 respectively. The measured and modeled peak enhancement data is plotted as a function of speckle decorrelation time and number of segments in the SLM in Fig. 4.

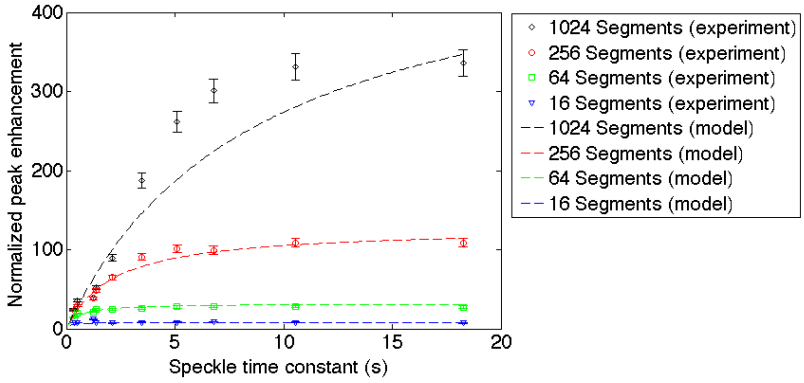

Fig. 4. Normalized peak enhancement as a function of speckle decorrelation time and number of independent segments in the SLM. Error bars correspond to the span of mean enhancement for three trials at each experimental condition.

For shorter speckle decorrelation times associated with fast-changing dynamic media, the advantage of additional segments in the SLM becomes increasingly less significant in the overall task of enhancing focus intensity. This is expected: the additional degrees of freedom enabled by more segments require proportionately longer time to cycle through a full set of

#168050 - $15.00 USD Received 9 May 2012; revised 7 Jun 2012; accepted 7 Jun 2012; published 20 Jun 2012

orthogonal Walsh coordinate optimizations. When the speckle decorrelation time is shorter than the time required to complete that set of optimizations, the advantages of additional orthogonal coordinates is substantially diminished. The results obtained experimentally here correspond well both qualitatively and quantitatively to analytical predictions proposed previously [26] for optimization through fluctuating media.

5. Discussion and conclusions

Controlling optical intensity enhancement through highly scattering media could have relevance to nonlinear microscopy for deep *in-vivo* brain tissue imaging [27]. In this important application, scattering of the focused incident beam strongly limits the achievable imaging depth. An optical control technique that could enhance focus intensity *inside* of a scattering medium would extend that achievable imaging depth. Whereas the experiments reported in this work achieve enhanced focus *outside* of the medium, the same technique could be used to optimize inside the medium in two-photon microscopy, with the two-photon excited signal used as optimization feedback. When the incident beam's focal intensity is increased, this two-photon excitation will also increase, in proportion to the *square* of the enhancement.

The controller has been demonstrated to be fast enough to achieve significant enhancement in focus through thick *ex vivo* tissue samples. Additional data are collected on media in which scattering mean free path and far-field speckle decorrelation times could be controlled. Optimization of focus through this controlled medium confirms a previously-proposed relationship [2] between the achievable intensity enhancement and the relevant system parameters: controller update rate, speckle decorrelation time, and number of independent mirror segments in the SLM.

The control bandwidth for the experiments described here was limited to 330Hz by the CMOS camera sensor frame rate. The SLM is capable of much higher update rates (>10kHz). For focus enhancement through dynamic media, a fast single-point sensor such as a PIN photodetector or a photomultiplier can take the place of the CMOS camera, enabling a potential thirty-fold decrease in the allowable speckle decorrelation time for a given enhancement value.

Acknowledgments

This work was supported by National Academies Keck Futures Initiative (NAKFI) grant number NFAKI-IS10 from the W.M. Keck Foundation. We are grateful to BMC for providing the SLM used in this work, and to Jerome Mertz and Jason Fleischer for helpful suggestions regarding our experiments. Professor Bifano acknowledges a financial interest in BMC.

#168050 - $15.00 USD Received 9 May 2012; revised 7 Jun 2012; accepted 7 Jun 2012; published 20 Jun 2012